Adaptive Drift Calibration of Accelerometers with Direct Velocity Measurements

Mike Rockwood[1] (Member IEEE), Bruce Wallace[1] (Sr Member IEEE), Rafik Goubran[1,2](Fellow IEEE), Frank Knoefel[1,2,3], Shawn Marshall[4]
[1]Systems and Computer Engineering
Carleton University, Ottawa, Canada
{mrockwood, wally, goubran, fknoefel}@sce.carleton.ca

[2]Bruyere Research Institute
[3]Faculty of Medicine
[4]Ottawa Hospital Research Institute,
University of Ottawa, Ottawa, Canada
smarshall@ottawahospital.on.ca

***Abstract*— The accelerometer has become one of the most popular sensors in recent years due to its low cost and the widespread availability of smart phones that now contain three axis accelerometers. This paper proposes an adaptive drift calibration technique for accelerometer signals, correcting higher sampling rate accelerometers using lower sampling rate velocity and position measurements. Specifically, this study made use of 40Hz sampled accelerometer signals captured by smart phones, and corrected them using two different 1Hz sampled velocity reference signals: a vehicle speed sensor and velocity from a Global Positioning System position sensor. The paper compares the performance of two error correction algorithms based on step and ramp shaped error correction delta functions. The ramp function was found to be susceptible to oscillation caused by high frequency noise, while the step function remains stable. The paper also shows that the GPS velocity signal has better performance over the dashboard vehicle velocity signal due to the higher frequency noise within the direct velocity signal.**

Keywords*— *Acceleration, Global Positioning System (GPS), Data Analytics, Adaptive Calibration

I. INTRODUCTION

Accelerometers have become extremely popular tools for data collection in recent years. They are less expensive, lower power, and offer much higher sensitivity than many other methods of measuring movement, such as the Global Positioning System (GPS). Additionally, they are widely available as they are a standard sensor included in all smart phones, which have been nearly ubiquitously adopted by the general public. They have been widely employed by many research groups for a wide variety of purposes, from detection of movement during sleep to robot control systems. One common application of accelerometers is to characterize human movement, as shown by Butala [1] and Gupta [2]. Calore [3] proposes an application of accelerometers for on board vehicle image correction and shows that calibration of the accelerometer is a key factor in performance.

Acquiring accurate measurements from accelerometer data presents a number of challenges. Firstly, accelerometers are very sensitive to vibration noise, secondly, they are often susceptible to baseline drift, and finally, they are prone to inaccuracies in all aspects of factory calibration and quality: offset, scaling, and orthogonality where the three axes are not perpendicular to each other. In addition to these physical limitations, in order to translate acceleration data into position or velocity data, it is necessary to integrate. This means any noise, drift, or even software rounding error will result in significant cumulative error problems over time, as shown in Fig. 1. While it has been shown by Handel [4] that acceleration signals can provide additional insight such as detection of gear shifts resulting in potential need for higher sampling rate and long term stable acceleration measurement.

A number of methods for resolving this problem have been proposed. Some, such as Silva [5], who proposes a polymer based fabrication technique for a three axis accelerometer, have worked on improving accelerometer manufacturing techniques and materials, while others have investigated post-manufacturing methods for improving the calibration of existing devices.

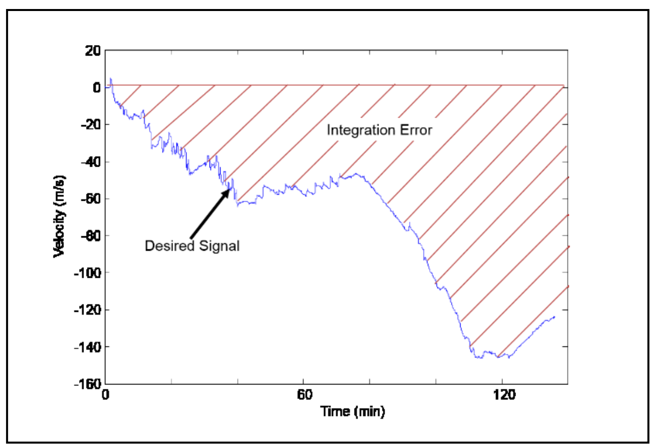

Fig. 1: Integration error over 135 minutes of driving data.

Techniques for accelerometer calibration have been reported by Frosio [6], who proposes an auto calibration technique for MEMS accelerometers using the gravity vector while the accelerometer is motionless. Timpson [7] proposes an external system for the calibration of an accelerometer. Guan [8] proposes an apparatus that can provide known accelerations for the laboratory calibration of accelerometers. Others, such as Beravs [9] and Won [10] have proposed algorithms that use robotic arms or similar to ensure precise accelerometer orientation during calibration. While these

This work was supported in part by the Natural Sciences and Engineering Research Council (NSERC). Candrive sensor provided by Candrive prospective study (www.candrive.ca) which is an interdisciplinary health related research program dedicated to improving the safety of elderly drivers funded by the Canadian Institutes of Health Research (CIHR)

978-1-4799-6144-6/15/$31.00 ©2015 IEEE

methods may work to improve accelerometer performance, they still present difficulties in that each requires the use of specialized external equipment, and none provide any assistance at all while the accelerometer is in use.

The application of accelerometers to the study of driving performance, particularly for assessing the abilities of older drivers is a potentially promising area of research. Marshall [11, 12], Eby [13], and Wallace [14, 15, 16] have proposed in-vehicle sensor systems that allow the recording of driving behaviors. These studies have shown that sensor equipment is capable of providing a clearer understanding of drivers' performance, but thus far, none of these studies have made use of accelerometer sensors with large user populations because of the challenges with the deployment and use of these sensors.

II. METHOD

A. Data Collection

Sensors to measure velocity and acceleration were deployed in one of the authors' vehicles. For measuring velocity, a Candrive Persentech OttoView-CD sensor [11, 12, 16] was provided by the Candrive project and deployed. It provides two measures of velocity:

- GPS: The Global Positioning System directly measures the vehicle position and it also provides a measure of velocity through calculation of the change in position over time.
- OBDII: The On Board Diagnostics Version II interface has been standard on all North American vehicles since 1996 and providing the dashboard vehicle velocity signal.
- The Candrive sensor records the readings of both of sensors at a f_{CD}=1Hz sampling rate.

For acceleration, three Blackerry Z10 smart phones, each containing three axis accelerometers, were used along with an application reported by Rockwood [17] that recorded the accelerometer readings. The accelerometers were sampled at f_{SP}=40Hz. Three smart phones were used so that multiple recordings of each of the test cases were available. The smart phones were positioned in the trials such that the vehicle motion was aligned with one axis of the accelerometer.

B. Measurement Challenge

Accelerometer use over longer periods of time is impacted by offsets and drift in the accelerometer readings [3]. This is shown in equation 1, where the measured accelerometer value has Gaussian noise (Z_a) and non-stationary drift component (d).

$$A_m[m] = A_a[m] + Z_a[m] + d[m] \quad (1)$$

The GPS and OBDII sensors provide two different measures of vehicle velocity and, as shown in equation 2, the actual velocity measure is assumed to also contain noise (Z_v).

$$V_m[n] = V_a[n] + Z_v[n] \quad (2)$$

In a system without noise or drift, the higher sampling rate acceleration signal (f_{SP}) can be integrated as shown in equation 3 to provide the actual velocity at f_{CD} sampling rate where the noise signal (Z_I) is introduced because of error associated with discrete signals and integration approximation and the decimation ratio (R) is provided by equation 4. The trapz function performs a trapezoidal integration of the set (w) of R $1/f_{SP}$ spaced acceleration samples between each velocity sample.

$$V_a[n] = V_a[n-1] + \mathrm{trapz}(A_a[w])/f_{SP} + Z_I[n] \quad (3)$$

$$\text{where } \mathrm{w} = R\mathrm{n} - (R-1){:}\,R\mathrm{n}$$

$$\mathrm{R} = {f_{SP}}/{f_{CD}} \quad (4)$$

But for a system with drift and noise, integrating each of the sets of R acceleration samples will introduce an error in the predicted velocity. The OBDII and GPS sensors each provide an independent reference measure of velocity at a lower sampling rate that can be used as a reference signal to adaptively correct the accelerometer readings.

C. Adaptive Correction

The method for adaptive correction of the accelerometer signals is shown in equation 5, where the predicted value for the velocity is calculated based on the previous measured reference velocity and the trapezoidal integration of the acceleration signals (A_c) that include all previous calculated corrections accounting for the higher sampling rate of the smart phone signals. From this, an error signal (ϵ) can be determined through the difference of the predicted velocity and the measured velocity from either the GPS or OBDII sensor.

$$V_p[n] = V_m[n-1] + \mathrm{trapz}(A_{c_{\mathrm{n}-1}}[w])/f_{SP} \quad (5)$$

$$\epsilon_{\mathrm{n}} = V_m[n] - V_p[n] \quad (6)$$

This error signal can then be used to iteratively update the correction to the acceleration signal through equation 7, where the current and all future acceleration values are updated based on a delta update function. Two different delta functions are analyzed as shown in equation 8 and 9. In equation 8, the update for the current window of R samples is flat, while in equation 9, the update is a ramp function. The step delta is an intuitive choice, but since the error being corrected included a drift component, the ramp shape was also investigated because it allows for the correction to grow across the window. In both cases, the delta (Δ) function is scaled so that it provides 100% correction while accounting for the over sampling of the acceleration signals. For the step update, the acceleration signals are all scaled by f_{SP} while the ramp has to be scaled by a factor that accounts for the oversampling and triangular shape.

$$A_{c_n}[m] = A_{c_{n-1}}[m] + \Delta[\mathrm{m}] * \epsilon_{\mathrm{n}}; \quad \mathrm{m} >= \mathrm{R(n\text{-}1)+1} \quad (7)$$

$$\Delta_{\mathrm{step}}[\mathrm{k}] = \mathrm{f_{SP}} \quad (8)$$

$$\begin{aligned} \Delta_{\mathrm{ramp}}[\mathrm{k}] &= \mathrm{k} * \mathrm{f_{SP}} * (2/(1+\mathrm{R})); \quad \mathrm{k}{=}1{:}\mathrm{R} \\ &= \mathrm{R} * \mathrm{f_{SP}} * (2/(1+\mathrm{R})); \quad \mathrm{k}>\mathrm{R} \end{aligned} \quad (9)$$

This adaptive correction algorithm is similar in approach to a traditional Kalman filter in that it performs a correction using a combination of similar sensors, as shown by Barrios [18], who corrected position estimates from velocity measures. These two approaches differ, however, in that the adaptive correction algorithm corrects the acceleration signal, while the Kalman filter would not, instead generating its output by "tuning out" erroneous measurements based on a comparison with a calculated expected value. In this way, the Kalman filter will handle sensor loss better (for instance the loss of GPS connectivity when entering a tunnel), but may lose information through attenuating sensor input.

D. Datasets

A total of 16 acceleration profiles were collected in which the vehicle accelerated from stopped to a maximum speed of between 50 and 80 kilometers per hour, and then returned to a full stop. The three smart phones were deployed in different orientations within the vehicle as summarized below:

- All three phones with top in the direction of travel.
- Two phones with bottom in the direction of travel and one phone with top in the direction of travel.
- All three phones with left side in the direction of travel.
- Two phones oriented with right side in the direction of travel and 1 phone with left side in the direction of travel.

For each of the above four configurations, four acceleration profiles were recorded on each of the three smart phones, providing three sets of 16 acceleration measurements.

E. Performance Measurement

The performance of the adaptive algorithm can be measured through three performance measures:

- Error signal average power
- Stability of calibrated acceleration and velocity signals.
- Correlation of the resulting acceleration signals.

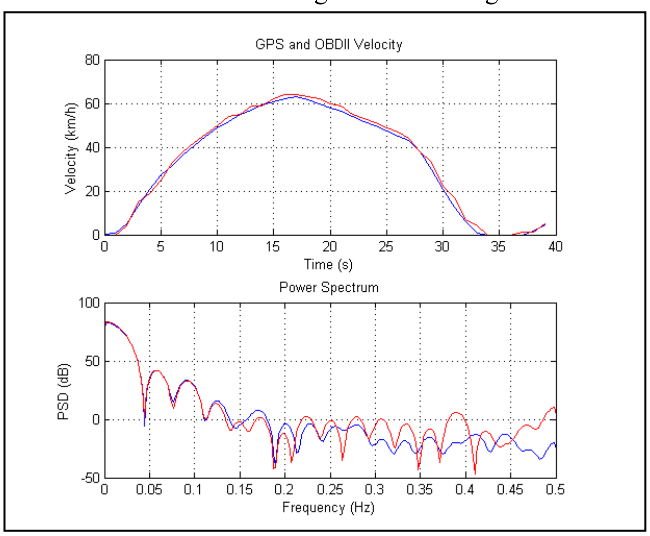

Fig. 2: Example acceleration/deceleration profile with the GPS sensor results in blue and the OBDII sensor results in red. The upper plot shows the time domain for the profile while the lower plot shows the frequency domain.

The correlation of three accelerometer signals for each profile is measured using equation 10 and 11 where *h[m]* and *k[m]* are the two acceleration profiles being compared.

$$R = \left(\frac{\sum_m h^*[m]k[m]}{\sqrt{E_h E_k}} \right) \tag{10}$$

$$where\ E_h = \sum_m (h[m])^2 \tag{11}$$

III. Experimental Results

A. Acceleration Calibration

Fig. 2 illustrates the difference between velocity profiles measured using the OBDII velocity sensor and the GPS position based velocity sensor. The upper plot shows the two measures of the profile in the time domain, while the lower plot shows the power spectrum for each measure. The similarity between the profiles is clear, but it is also clear in both the upper and lower plots that the OBDII signal contains a small amount of high frequency information or noise that is missing from the GPS calculated velocity.

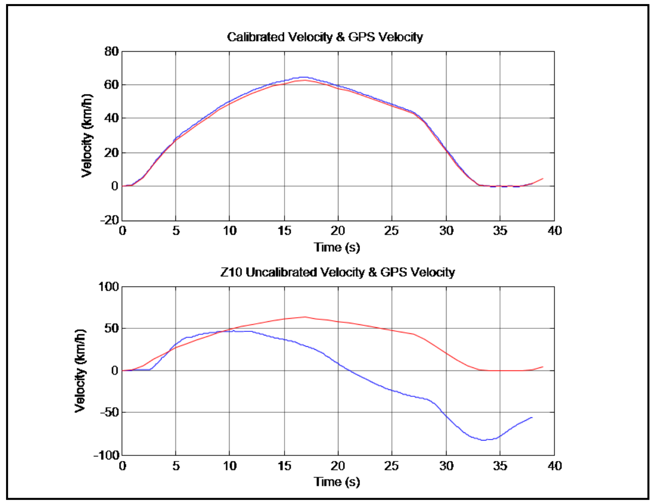

Fig. 3: Comparison of the velocity calculated by the accelerometer before and after calibration. Accelerometer calculated velocity is shown in blue, and the reference GPS velocity is shown in red.

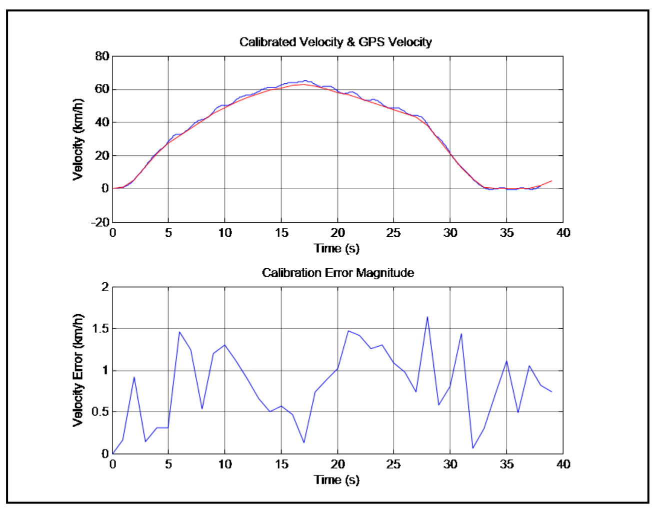

Fig. 4: The upper plot shows an example acceleration/deceleration profile using the ramp-shaped delta function (shown in blue) compared to the reference GPS velocity measure (shown in red). The lower plot shows the magnitude of the error calculated by the algorithm.

Fig. 3 shows a comparison between the achievable accelerometer correction and the uncorrected signal. Even within a 40 second timeframe, the effect of the drift is visible, as the resulting acceleration profile is significantly affected and instead of returning to zero velocity, the car has a negative velocity. Fig. 4 shows the effect of using the ramp shaped delta function in the correction algorithm. The difference in the ramp delta function results in overcorrection and oscillations, as well as a sharp increase in the measured error.

Fig. 5 shows the effect of the ramp delta function to correct the accelerometer using the OBDII as a reference velocity. Here, the high frequency components of the OBDII measured velocity lead to significant oscillation in the resulting error signal. In both cases, the ramp function leads to an over correction on the subsequent acceleration values leading to the unacceptable oscillation in the corrected velocity signals.

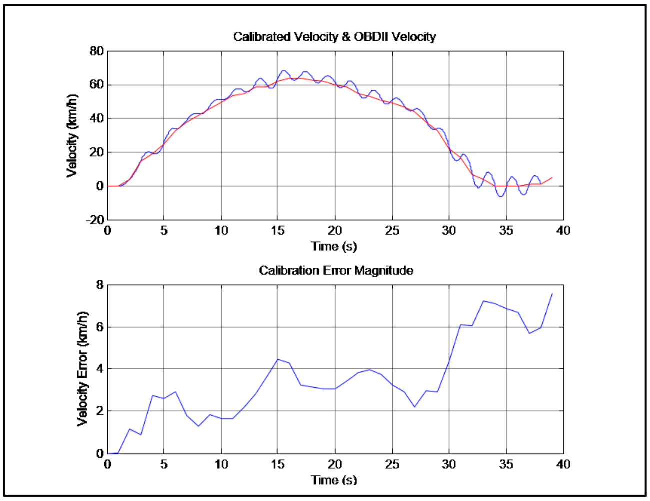

Fig. 5: The upper plot shows an example acceleration/deceleration profile using the ramp-shaped delta function (shown in blue) compared to the reference OBDII velocity measure (shown in red). The lower plot shows the magnitude of the error calculated by the algorithm.

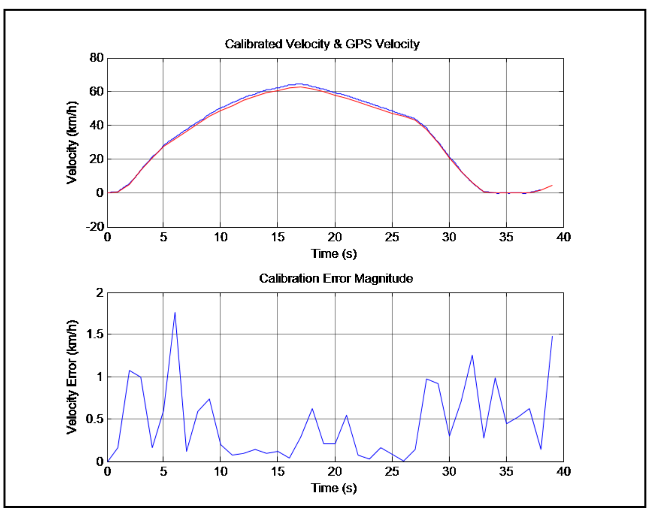

Fig. 6: The upper plot shows an example acceleration/deceleration profile using the step-shaped delta function (shown in blue) compared to the reference GPS velocity measure (shown in red). The lower plot shows the magnitude of the error calculated by the algorithm.

Fig. 6 shows the step shaped delta function applied to the correction algorithm, using the GPS derived velocity as the reference. This delta function improves the performance of the correction algorithm considerably, nearly eliminating the oscillation effect. Fig. 7 shows the correction algorithm results using the same step delta function as above, but with the OBDII measured velocity as a reference. Here, it is once again possible to see a small oscillation effect from the higher frequency component of the reference velocity measure.

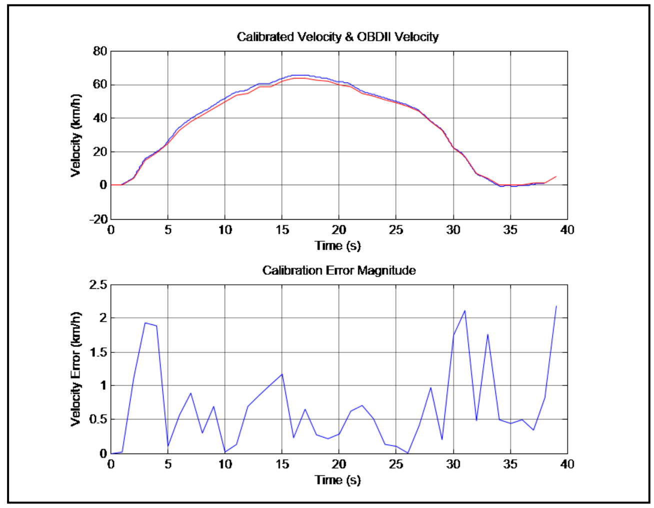

Fig. 7: The upper plot shows an example acceleration/deceleration profile using the step-shaped delta function (shown in blue) compared to the reference OBDII velocity measure (shown in red). The lower plot shows the magnitude of the error calculated by the algorithm.

B. Error Signal Power

TABLE I. A SUMMARY OF THE AVERAGE TOTAL ENERGY OF THE VELOCITY ERROR IN EACH ACCELERATION/DECELERATION PROFILE, MEASURED USING STEP AND RAMP DELTAS FOR BOTH THE GPS AND OBDII REFERENCE VOLTAGES.

		GPS		OBDII	
		step	ramp	step	ramp
Acc A	Min	0.460	0.593	0.792	3.002
	Max	0.751	1.518	1.303	9.639
	Mean	0.574	1.051	1.090	5.404
	Stdev	0.087	0.297	0.151	1.852
Acc B	Min	0.448	0.687	0.810	3.238
	Max	0.748	1.974	1.366	10.338
	Mean	0.589	1.132	1.106	5.546
	Stdev	0.086	0.366	0.168	1.764
Acc C	Min	0.399	0.411	0.747	3.472
	Max	0.756	1.832	1.428	8.650
	Mean	0.532	0.979	1.064	5.585
	Stdev	0.087	0.374	0.153	1.456

Table I shows the minimum, maximum, mean, and standard deviation of the average total energy of the error for each acceleration/deceleration profiles. The mean error energy using the GPS velocity reference is lower than for the OBDII velocity reference, and the step delta error energy is always lower than the ramp delta. The high quality of the resulting velocity signals that can be derived from the step delta corrected accelerometer signal is shown by the average Signal to Error Ratio of 38.1 dB for the GPS reference and the reduced performance of 32.6 dB for the OBDII reference.

C. Correlation of Corrected Acceleration Signals

Tables II and III contain the minimum, maximum, mean, and standard deviation of the correlation between the corrected and uncorrected measures of acceleration. The corrected accelerations have a significantly higher mean and much narrower standard deviation showing the improvements that have been achieved when the accelerations are recalibrated using the GPS reference and the step delta function.

TABLE II. SUMMARY OF THE UNCORRECTED ACCELERATION SENSOR CORRELATION DATA FOR EACH OF THE SMART PHONE ACCELERATION PROFILES.

		Acc A	Acc B	Acc C
Acc A	**Max**		0.884	0.896
	Mean		0.833	0.850
	Min		0.756	0.795
	StDev		0.037	0.034
Acc B	**Max**	0.884		0.908
	Mean	0.833		0.852
	Min	0.756		0.722
	StDev	0.037		0.045
Acc C	**Max**	0.896	0.908	
	Mean	0.850	0.852	
	Min	0.795	0.722	
	StDev	0.034	0.045	

TABLE III. SUMMARY OF THE CORRECTED ACCELERATION SENSOR CORRELATION DATA FOR EACH OF THE SMART PHONE ACCELERATION PROFILES USING THE GPS VELOCITY REFERENCE AND STEP DELTA FUNCTION.

		Acc A	Acc B	Acc C
Acc A	**Max**		0.978	0.966
	Mean		0.967	0.954
	Min		0.957	0.935
	StDev		0.007	0.009
Acc B	**Max**	0.978		0.967
	Mean	0.967		0.951
	Min	0.957		0.934
	StDev	0.007		0.009
Acc C	**Max**	0.966	0.967	
	Mean	0.954	0.951	
	Min	0.935	0.934	
	StDev	0.009	0.009	

IV. DISCUSSION

This paper has shown that using a reference velocity signal, such as a direct velocity measurement through an OBDII interface or a velocity derived from a GPS sensor, allows dynamic drift correction of accelerometer data, even over long time periods. This correction allows the use of accelerometers in continuous monitoring of driving behavior. The paper has also shown that a ramp based delta function causes unacceptable oscillations in the calibrated signal while the step delta function provides improved performance.

Accelerometer sensors that are very low power are now available, and through the use of calibration techniques, they can be deployed in sensor solutions where directly measuring position requires high power consumption (such as when using a GPS) to allow a higher sampling rate while still optimizing battery use. The use of dynamic calibration will also allow for the longer term deployment and measurements over longer periods of time.

Future areas for exploration include the extension of the dynamic calibration algorithm to include adaptive scale calibration to account for any variable scaling issues with the accelerometer signals over long duration recording.

REFERENCES

[1] P. M. Butala, Y. Zhang, T. D. C. Little, "Wireless system for monitoring and real-time classification of functional activity," in proc. *International Conference on Communications Systems and Networks (COMSNETS)*, pp. 3-7, 2012.

[2] P. Gupta, T. Dallas, "Feature Selection and Activity Recognition System Using a Single Triaxial Accelerometer," *Biomedical Engineering, IEEE Transactions on*, vol. 61, no. 6, pp. 1780-86, Jun. 2014.

[3] E, Calore, F. Pedersini, I. Frosio, "Accelerometer based horizon and keystone perspective correction," in proc. *Instrumentation and Measurement Technology Conference (I2MTC), 2012 IEEE International,* pp. 205-209, 2012.

[4] P. Handel, "Discounted least-squares gearshift detection using accelerometer data." *Instrumentation and Measurement, IEEE Transactions on,* vol 58: pp. 3953-3958, 2009.

[5] C. Silva, J. Pontes, J. Viana, L. Rocha, J. Gaspar, "A fully integrated three-axis thermal accelerometer," in proc. *Instrumentation and Measurement Technology Conference (I2MTC), 2013 IEEE International*, pp. 963-966, 2013.

[6] I. Frosio, F. Pedersini, N. Alberto Borghese, "Autocalibration of MEMS accelerometers," *Instrumentation and Measurement, IEEE Transactions on*, vol *58*(6), pp. 2034-2041, 2009.

[7] E. Timpson, T. Engel, "Calibrating accelerometers using an Electromagnetic Launcher," in proc. *Instrumentation and Measurement Technology Conference (I2MTC), 2012 IEEE International*, pp. 1027-1032, 2012.

[8] W. Guan, X. Meng, X. Dong, "Calibration of accelerometer with multicomponent inputs," in proc. *Instrumentation and Measurement Technology Conference (I2MTC), 2014 IEEE International,* pp. 16-19, 2014.

[9] T. Beravs, J. Podobnik, M. Munih, "Three-Axial Accelerometer Calibration Using Kalman Filter Covariance Matrix for Online Estimation of Optimal Sensor Orientation," *Instrumentation and Measurement, IEEE Transactions on* , vol.61, no.9, pp. 2501-2511, 2012.

[10] S. Won, F. Golnaraghi, "A Triaxial Accelerometer Calibration Method Using a Mathematical Model," *Instrumentation and Measurement, IEEE Transactions on* , vol.59, no.8, pp. 2144-2153, 2010.

[11] S. Marshall, et al. "Protocol for Candrive II/Ozcandrive, a multicentre prospective older driver cohort study," *Accident Analysis & Prevention,* vol. 61, pp. 245–252, 2013.

[12] S. Marshall, et al. "The Canadian Safe Driving Study–phase I pilot: Examining potential logistical barriers to the full cohort study," *Accident Analysis & Prevention*, vol. 61, pp. 236–244, 2013.

[13] D. Eby, et al. "Driving behaviors in early stage dementia: A study using in-vehicle technology," *Accident Analysis & Prevention*, vol. 49, pp. 330-337, 2012.

[14] R. Wallace, R. Goubran, F Knoefel, "Measurement of Driving Routes and Correlation to Optimal Navigation Paths," in proc. *International Instrumentation and Measuremnt Conference (I2MTC), 2013 IEEE*, pp. 1465-1470, 2013.

[15] R. Wallace, R. Goubran, F Knoefel, "Measurement of Signal Use and Vehicle Turns as Indication of Driver Cognition," in proc. *IEEE Engineering in Medicine and Biology Society (EMBC), 36th Annual International Conference of the*, pp. 3747-3750, 2014.

[16] R. Wallace, R. Goubran, F. Knoefel, S. Marshall, M. Porter, "Measuring Variation in Driving Habits Between Drivers," in proc. *Medical Measurements and Applications (MeMeA), 2014 IEEE International Symposium on*, pp. 29-34, 2014.

[17] M. Rockwood, V. Joshi, K. Sullivan, R. Goubran, "Using a Real-Time Operating System for Multitasking in Remote Patient Monitoring," in proc. *Medical Measurements and Applications (MeMeA), 2014 IEEE International Symposium on*, pp. 475-479, 2014.

[18] C. Barrios, Y. Motai, "Improving Estimation of Vehicle's Trajectory Using the Latest Global Positioning System With Kalman Filtering," *Instrumentation and Measurement, IEEE Transactions on* , vol. 60, no. 12, pp. 3747-3755, 2011.